Developmental Cell, Volume *56*

Supplemental information

Formation of polarized contractile interfaces by self-organized Toll-8/Cirl GPCR asymmetry

Jules Lavalou, Qiyan Mao, Stefan Harmansa, Stephen Kerridge, Annemarie C. Lellouch, Jean-Marc Philippe, Stephane Audebert, Luc Camoin, and Thomas Lecuit

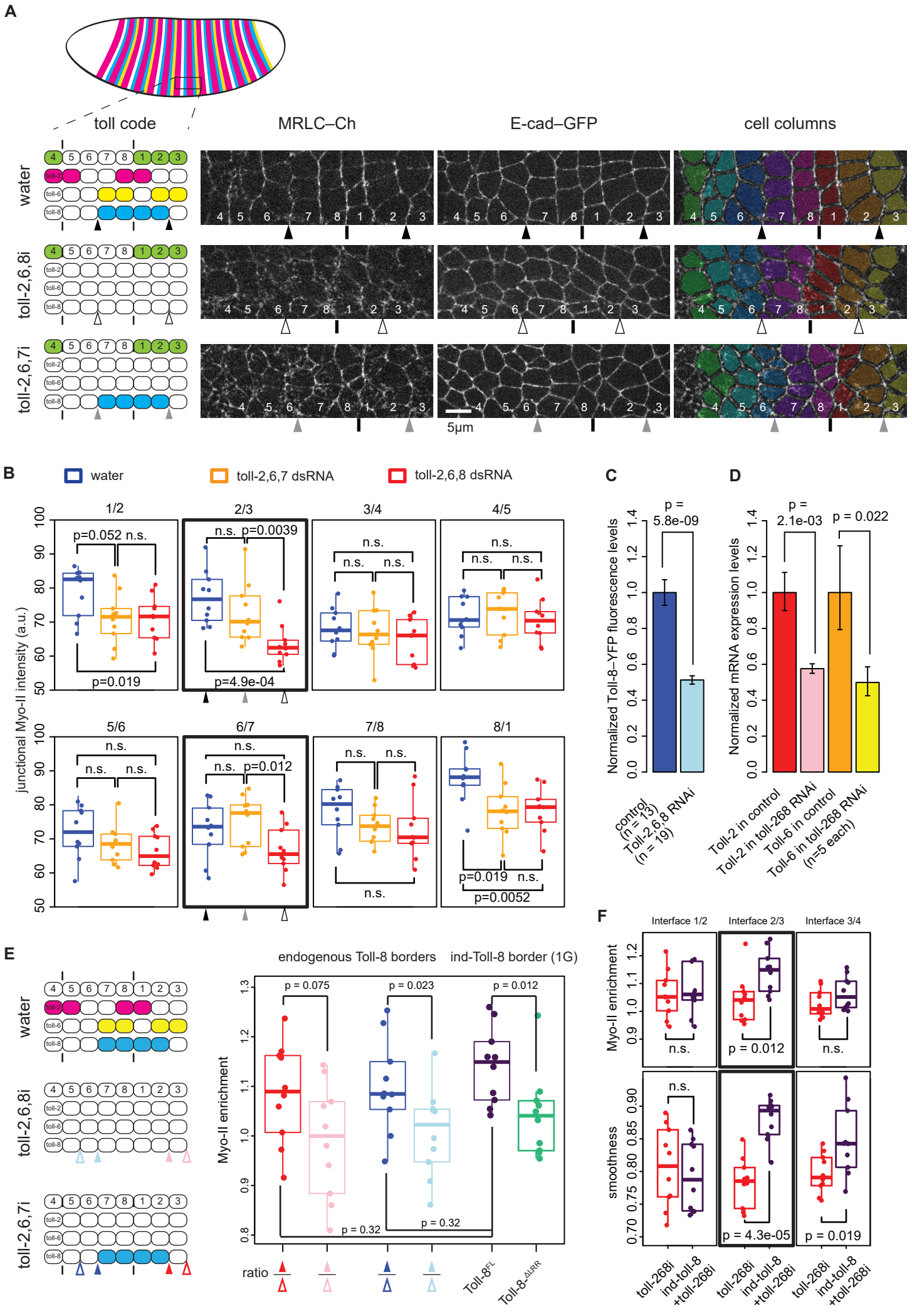
A
toll code
MRLC–Ch
E-cad–GFP
cell columns
water
toll-2,6,8i
toll-2,6,7i
5µm
B
water
toll-2,6,7 dsRNA
toll-2,6,8 dsRNA
junctional Myo-II intensity (a.u.)
1/2
2/3
3/4
4/5
5/6
6/7
7/8
8/1
p=0.052 n.s.
p=0.019
n.s. p=0.0039
p=4.9e-04
n.s.
p=0.012
p=0.019 n.s.
p=0.0052
C
Normalized Toll-8–YFP fluorescence levels
p = 5.8e-09
control (n = 13)
Toll-2,6,8 RNAi (n = 19)
D
Normalized mRNA expression levels
p = 2.1e-03
p = 0.022
Toll-2 in control
Toll-2 in toll-268 RNAi
Toll-6 in control
Toll-6 in toll-268 RNAi
(n=5 each)
E
endogenous Toll-8 borders
ind-Toll-8 border (1G)
Myo-II enrichment
p = 0.075
p = 0.023
p = 0.012
p = 0.32
p = 0.32
ratio
Toll-8FL
Toll-8ΔLRR
F
Interface 1/2
Interface 2/3
Interface 3/4
Myo-II enrichment
smoothness
n.s.
p = 0.012
p = 4.3e-05
p = 0.019
toll-268i
ind-toll-8 +toll-268i

Figure S1. Endogenous Toll-8 is able to enrich Myo-II at its expression boundaries independent of Toll-2,6 (related to Figure 1).

(A) Schematics of endogenous Toll-2,6,8 expression in embryos under various conditions (top left). Cell columns 1-4: odd parasegments (eve–YFP+, green in the schematics); 5-8: even parasegment (eve–YFP-). Arrowheads show the two boundaries of Toll-8 expression at positions 2/3 and 6/7. See methods for details. Still images from time lapse movies of stage 7 to early stage 8 embryos injected with water (top), dsRNAs against Toll-2,6,8 (middle) and dsRNAs against Toll-2,6,7 (bottom). Note that Toll-7 is not expressed during germband extension. Triple Toll-2,6,7 RNAi was performed to keep the total load of dsRNA comparable to the triple Toll-2,6,8 RNAi condition. Pseudo colors represent cell columns (right). In all panels, vertical bars represent parasegment boundaries where Myo-II is enriched despite of Toll-2,6,8 knockdowns. Arrowheads demark boundaries of the Toll-8 expression domain in embryos injected with water (black), dsRNAs against Toll-2,6,8 (white) or Toll-2,6,7 (grey), where Myo-II is enriched in the sole presence of Toll-8 (bottom).

(B) Quantifications of junctional Myo-II levels at indicated interfaces in embryos injected with water (blue, n=10), dsRNAs against Toll-2,6,7 (orange, n=10) and dsRNAs against Toll-2,6,8 (red, n=10). Black, white and grey arrowheads show quantifications of representative interfaces highlighted in (A).

(C) BAC-Toll-8-YFP (Paré et al., 2014) fluorescence levels in control embryos or in embryos injected with dsRNAs against Toll-2,6,8.

(D) Normalized mRNA expression levels obtained by RT-qPCR for Toll-2 and Toll-6 in control embryos or in embryos injected with dsRNAs against Toll-2,6,8. Toll-2,6,8 RNAi leads to a significant reduction of the expression of all three Toll receptors in the embryo.

(E) Quantification of Myo-II enrichment ratio at the endogenous boundary of the Toll-8 expression domain (interfaces 2/3, n=10; and 6/7, n=10) compared with Myo-II enrichment ratio at the ventral borders of ind-Toll-8 (as reported in Figure 1G). Myo-II enrichment ratios at both endogenous Toll-8 borders are not significantly different from the ind-Toll-8 ventral border. Myo-II is more enriched when Toll-8 is asymmetrically expressed than when Toll-8 is absent from both sides.

(F) Additional quantifications for Figures 1F-H. Quantifications of junctional Myo-II enrichment (top) and boundary smoothness (bottom) at interfaces 1/2 (left, interfaces within the ind-Toll-8^{FL}–HA domain), 2/3 (center, boundary interfaces) and 3/4 (right, interfaces within the wild-type tissue).

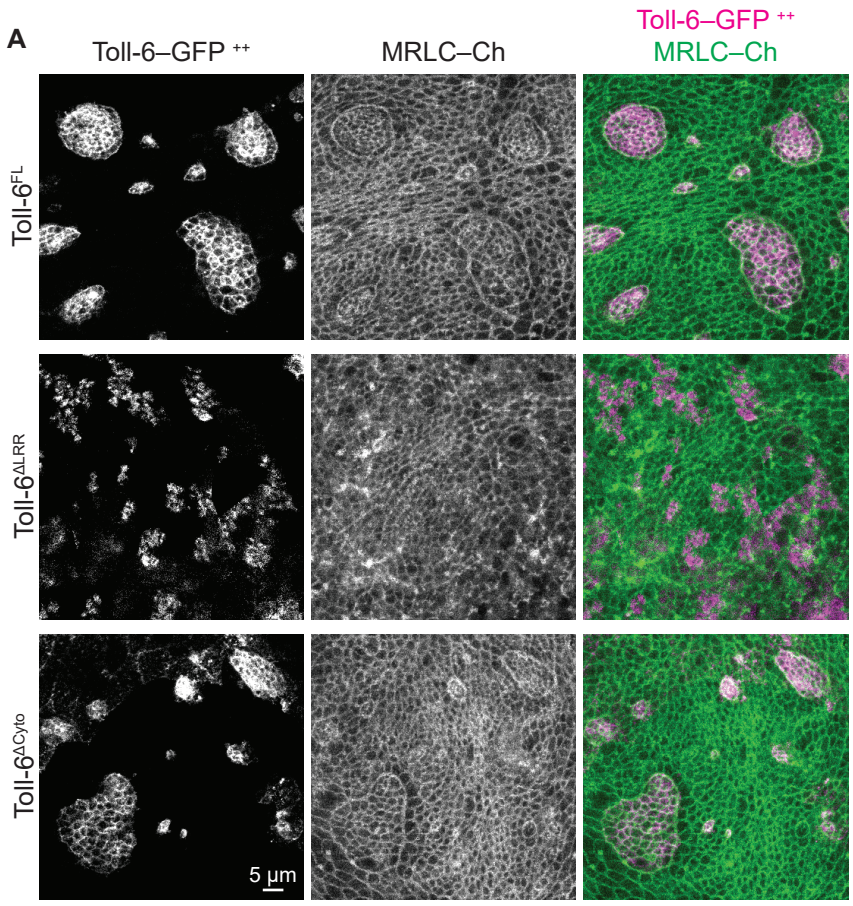
A
Toll-6–GFP ++
MRLC–Ch
Toll-6–GFP ++
MRLC–Ch
Toll-6FL
Toll-6ΔLRR
Toll-6ΔCyto
5 µm

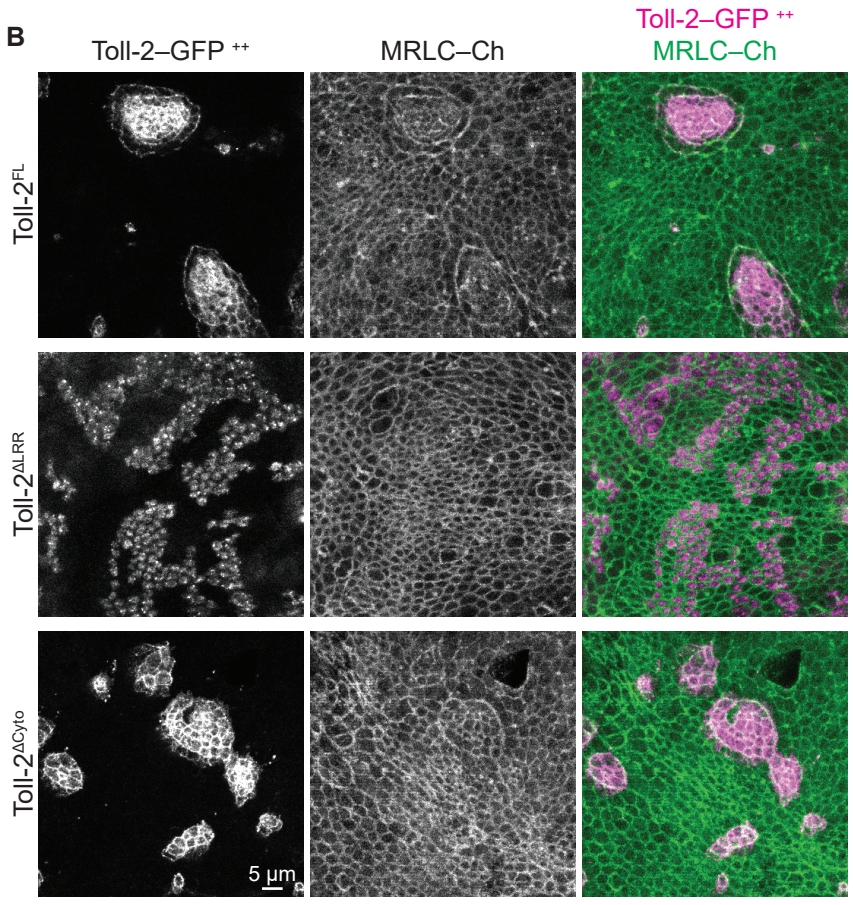
B
Toll-2–GFP ++
MRLC–Ch
Toll-2–GFP ++
MRLC–Ch
Toll-2FL
Toll-2ΔLRR
Toll-2ΔCyto
5 µm

Figure S2. Asymmetric expression of Toll-6 and Toll-2 without their cytoplasmic tails leads to Myo-II enrichment in wing discs (related to Figure 2).

(A) Fixed Toll-6–GFP and MRLC–Ch signals from wing disc clones overexpressing full length Toll-6 (Toll-6^{FL}, top), Toll-6 with the extracellular LRRs removed (Toll-$6^{\Delta LRR}$, middle), or Toll-6 with the intracellular cytoplasmic tail removed (Toll-$6^{\Delta Cyto}$, bottom). Myo-II enrichment requires the extracellular LRRs but not the cytoplasmic tail of Toll-6.

(B) Fixed Toll-2–GFP and MRLC–Ch signals from wing disc clones overexpressing full length Toll-2 (Toll-2^{FL}, top), Toll-2 with the extracellular LRRs removed (Toll-$2^{\Delta LRR}$, middle), or Toll-2 with the intracellular cytoplasmic tail removed (Toll-$2^{\Delta Cyto}$, bottom). Myo-II enrichment requires the extracellular LRRs but not the cytoplasmic tail of Toll-2.

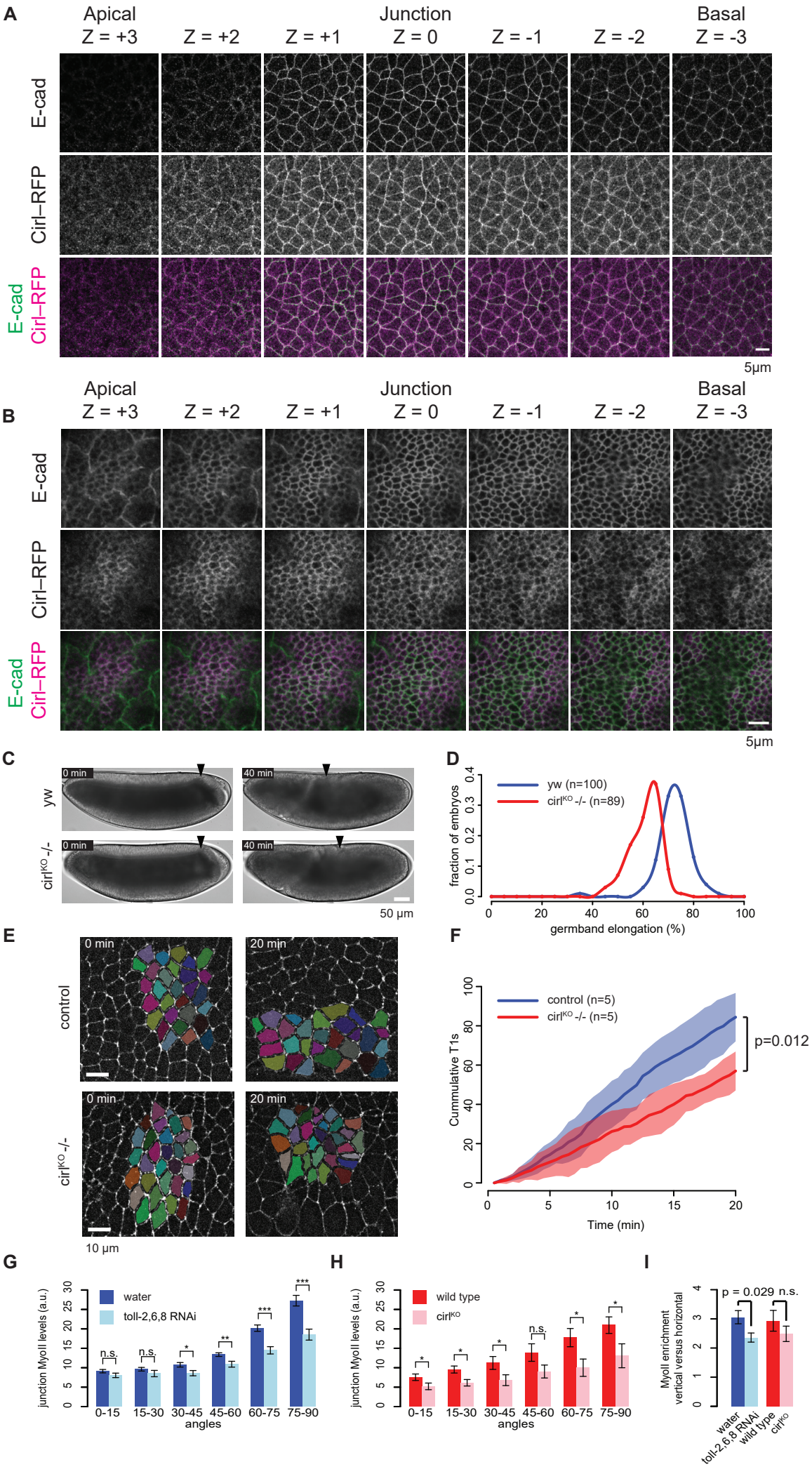
A
Apical
Junction
Basal
Z = +3
Z = +2
Z = +1
Z = 0
Z = -1
Z = -2
Z = -3
E-cad
Cirl–RFP
E-cad
Cirl–RFP
5µm
B
Apical
Junction
Basal
Z = +3
Z = +2
Z = +1
Z = 0
Z = -1
Z = -2
Z = -3
E-cad
Cirl–RFP
E-cad
Cirl–RFP
5µm
C
yw
cirlKO -/-
0 min
40 min
0 min
40 min
50 µm
D
yw (n=100)
cirlKO -/- (n=89)
fraction of embryos
germband elongation (%)
E
control
cirlKO -/-
0 min
20 min
0 min
20 min
10 µm
F
control (n=5)
cirlKO -/- (n=5)
p=0.012
Cummulative T1s
Time (min)
G
water
toll-2,6,8 RNAi
junction MyoII levels (a.u.)
n.s.
n.s.
*
**
***
***
0-15
15-30
30-45
45-60
60-75
75-90
angles
H
wild type
cirlKO
junction MyoII levels (a.u.)
*
*
*
n.s.
*
*
0-15
15-30
30-45
45-60
60-75
75-90
angles
I
Myoll enrichment vertical versus horizontal
p = 0.029 n.s.
water
toll-2,6,8 RNAi
wild type
cirlKO

Figure S3. Localization of Cirl in the *Drosophila* embryonic germband and wing disc cells, and its requirement in embryonic axis extension and cell intercalations (related to Figure 3).

(A) Anti E-cad (green) and anti Cirl–RFP (magenta) signals in the ectoderm epithelium in stage 7 *Drosophila* embryos. Sequential Z planes are shown from apical (left) to basal (right). Step size: 0.38 µm.

(B) Anti E-cad (green) and anti Cirl–RFP (magenta) signals in the wing disc pouch epithelium. Sequential Z planes are shown from apical (left) to basal (right). Step size: 0.25 µm. In both (A) and (B), Cirl–RFP is localized at cell-cell interfaces around adherens junctions.

(C) Axial extension at 0 and 40 minutes in *yw* (top, n=100) and $cirl^{KO}$ -/- (bottom, n=89) embryos. 0 min is defined as the beginning of axial extension. Arrowheads denote the dorsal edge of the posterior midgut primordium. Axial extension is slowed down in the absence of *cirl*.

(D) Histogram of axial extension for *yw* (blue, n=100) and $cirl^{KO}$ -/- (red, n=89) embryos for the conditions shown in (C).

(E) Still images from time lapse movies in *wt* (top, *n*=5) or $cirl^{KO}$ -/- (bottom, *n*=5) embryos. LifeAct–Ch marks cell outlines. Pseudo colors mark tracked cells. 0 min is defined as the beginning of axial extension.

(F) Cumulative numbers of T1 transitions in *wt* (blue, *n*=5) or $cirl^{KO}$ -/- (red, *n*=5) embryos for conditions shown in (E). Solid lines represent mean values, shaded areas represent standard deviation. *p*-value is calculated for total numbers of T1 transitions at the end of 20 minutes between *wt* and $cirl^{KO}$ -/- embryos.

(G and H) Junctional Myo-II levels binned by junction orientations (0-15°: horizontal junctions; 75-90°: vertical junctions) in water (dark blue, *n*=10) and Toll-2,6,8 dsRNA (light blue, *n*=10) injected embryos (G), and in wild type (dark red, *n*=8) and $cirl^{KO}$ (light red, *n*=8) embryos (H). *: $p < 0.05$; **: $p < 0.01$; ***: $p < 0.001$; n.s.: $p > 0.05$.

(I) Myo-II amplitude of polarity calculated as the enrichment ratio of vertical junctions (angles 75-90) over horizontal junctions (angles 0-15) for conditions shown in (G) and (H).

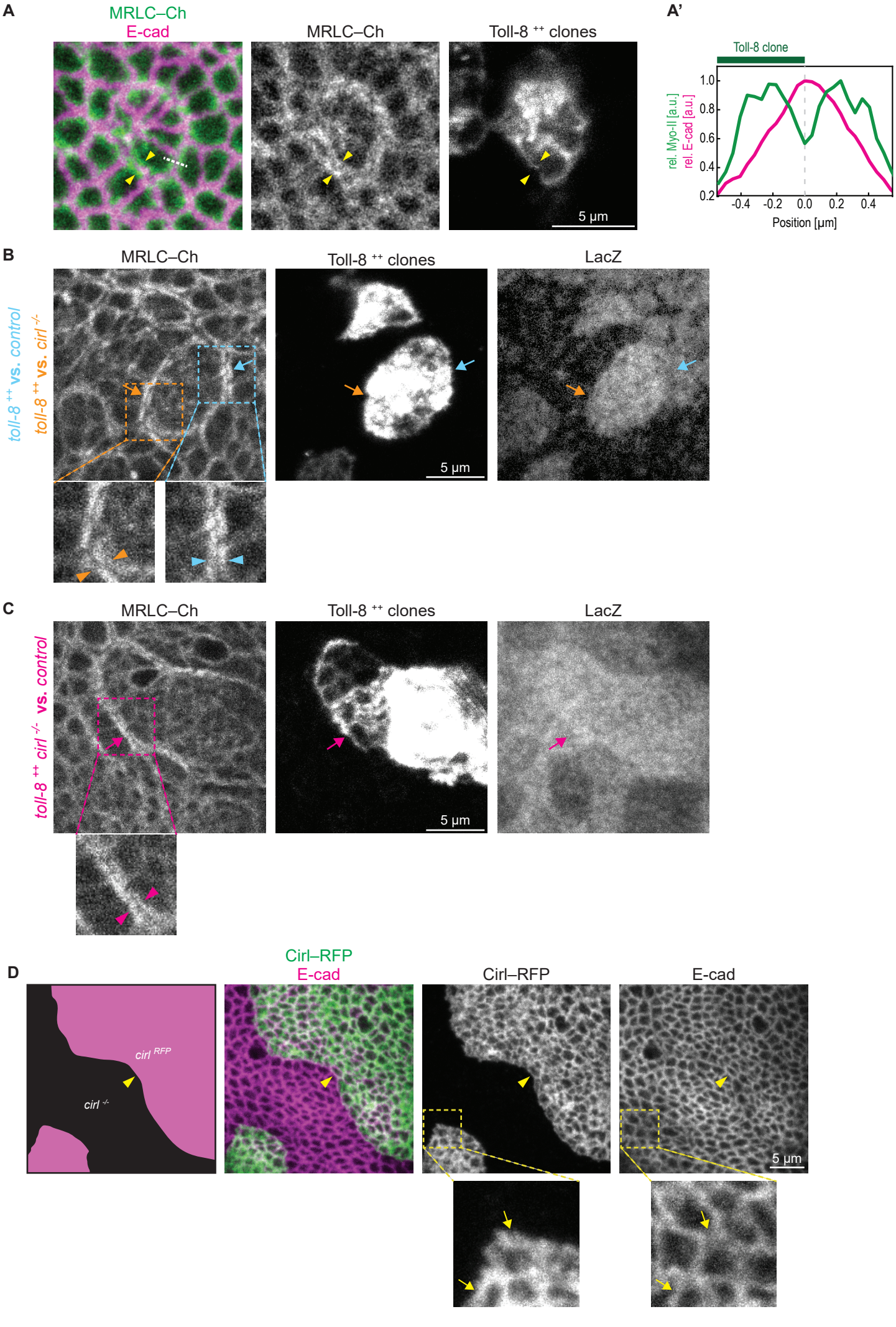
A
MRLC–Ch
E-cad
MRLC–Ch
Toll-8 ++ clones
5 µm
A'
Toll-8 clone
rel. Myo-II [a.u.]
rel. E-cad [a.u.]
1.0
0.8
0.6
0.4
0.2
-0.4
-0.2
0.0
0.2
0.4
Position [µm]
B
MRLC–Ch
Toll-8 ++ clones
LacZ
toll-8 ++ vs. control
toll-8 ++ vs. cirl -/-
5 µm
C
MRLC–Ch
Toll-8 ++ clones
LacZ
toll-8 ++ cirl -/- vs. control
5 µm
D
Cirl–RFP
E-cad
cirl RFP
cirl -/-
Cirl–RFP
E-cad
5 µm

Figure S4. Myo-II is enriched on both sides of the Toll-8 expression boundary (related to Figure 4).

(A) Fixed MRLC–Ch, E-cad and Toll-8–YFP signals from wing disc clones overexpressing Toll-8. Myo-II is enriched on both sides of the boundary of the clone. (A') shows the intensity profile quantified along the dashed white line in (A).

(B) Myo-II signals in MARCM clones in the wing disc where cells overexpressing Toll-8–YFP (*toll-8* $^{++}$, *lacZ* $^{+/+}$, green in Figure 4A) are juxtaposed with control cells heterozygous (*cirl* $^{+/-}$, *lacZ* $^{+/-}$, blue in Figure 4A, cyan arrow) or null mutant (*cirl* $^{-/-}$, *lacZ* $^{-/-}$, black in Figure 4A, orange arrow) for *cirl*. The cyan and orange arrowheads on the zoomed images indicate Myo-II enrichment on both sides of clone boundaries (related to Figure 4A).

(C) MARCM clones in the wing disc. Myo-II is enriched at clone boundaries (magenta arrow) where cells overexpressing Toll-8–YFP and null mutant for *cirl* (*toll-8* $^{++}$, *cirl* $^{-/-}$, *lacZ* $^{+/+}$, green in Figure 4B) are juxtaposed with cells heterozygous (*cirl* $^{+/-}$, *lacZ* $^{+/-}$ in blue in Figure 4B) or *wild-type* (*cirl* $^{+/+}$, *lacZ* $^{-/-}$ in black in Figure 4B) for *cirl*. The magenta arrowheads on the zoomed image mark Myo-II enrichment on both sides of the clone boundary (related to Figure 4B).

(D) Cirl–RFP is still localized in wild-type cell interfaces in contact with *cirl* mutant cells (arrowheads and arrows).

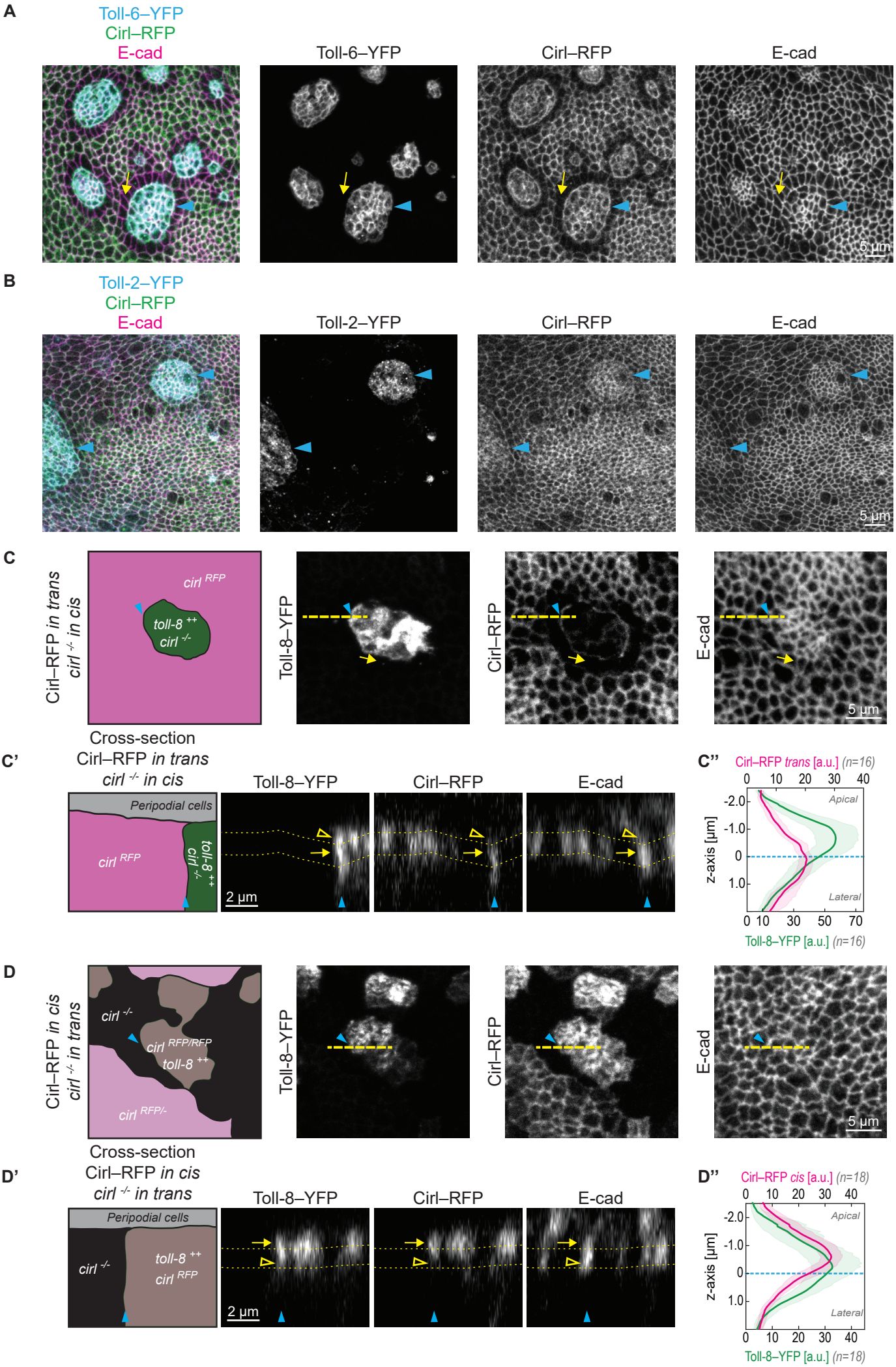
A
Toll-6–YFP
Cirl–RFP
E-cad
Toll-6–YFP
Cirl–RFP
E-cad
5 µm
B
Toll-2–YFP
Cirl–RFP
E-cad
Toll-2–YFP
Cirl–RFP
E-cad
5 µm
C
Cirl–RFP in trans
cirl -/- in cis
cirl RFP
toll-8 ++
cirl -/-
Toll-8–YFP
Cirl–RFP
E-cad
5 µm
Cross-section
Cirl–RFP in trans
cirl -/- in cis
Peripodial cells
cirl RFP
toll-8 ++
cirl -/-
Toll-8–YFP
Cirl–RFP
E-cad
2 µm
C''
Cirl–RFP trans [a.u.] (n=16)
0 10 20 30 40
-2.0
-1.0
0
1.0
z-axis [µm]
Apical
Lateral
0 10 30 50 70
Toll-8–YFP [a.u.] (n=16)
D
Cirl–RFP in cis
cirl -/- in trans
cirl -/-
cirl RFP/RFP
toll-8 ++
cirl RFP/-
Toll-8–YFP
Cirl–RFP
E-cad
5 µm
Cross-section
Cirl–RFP in cis
cirl -/- in trans
Peripodial cells
cirl -/-
toll-8 ++
cirl RFP
Toll-8–YFP
Cirl–RFP
E-cad
2 µm
D''
Cirl–RFP cis [a.u.] (n=18)
0 10 20 30 40
-2.0
-1.0
0
1.0
z-axis [µm]
Apical
Lateral
0 10 20 30 40
Toll-8–YFP [a.u.] (n=18)

Figure S5. Effect of Toll-6 and Toll-2 overexpression on Cirl distribution in the wing disc (related to Figure 5).

Blue arrowheads indicate clone boundaries in all panels.

(A) Toll-6–YFP overexpressing clone in a Cirl–RFP wing disc. Cirl–RFP is depleted from junctions orthogonal to the clone boundary (arrow).

(B) Toll-2–YFP overexpressing clone in a Cirl–RFP wing disc. Cirl–RFP localization is not affected by Toll-2 overexpression.

(C) Same experimental setup as in Figure 5B, with the exception that *cirl* is null mutant instead of untagged in Toll-8 overexpressing clones (*toll-8* $^{++}$, *cirl* $^{-/-}$ in green). Planar polarity of Cirl in wild-type cells neighboring Toll-8 overexpressing clones is not disturbed by the absence of Cirl inside the clones. (C') Optical cross-section (dashed line in (C)) shows Cirl–RFP enrichment at the junctional plane (yellow arrow), quantified in (C'').

(D) Same experimental setup as in Figure 5C, with the exception that *cirl* is null mutant instead of untagged in cells facing Toll-8 overexpressing clones (*cirl* $^{-/-}$ in black). (D') Optical cross-section (dashed line in (D)) shows Cirl–RFP enrichment above the junctional plane (yellow arrow), quantified in (D'').

Error bands indicate the 95% confidence interval in (C'') and (D'').

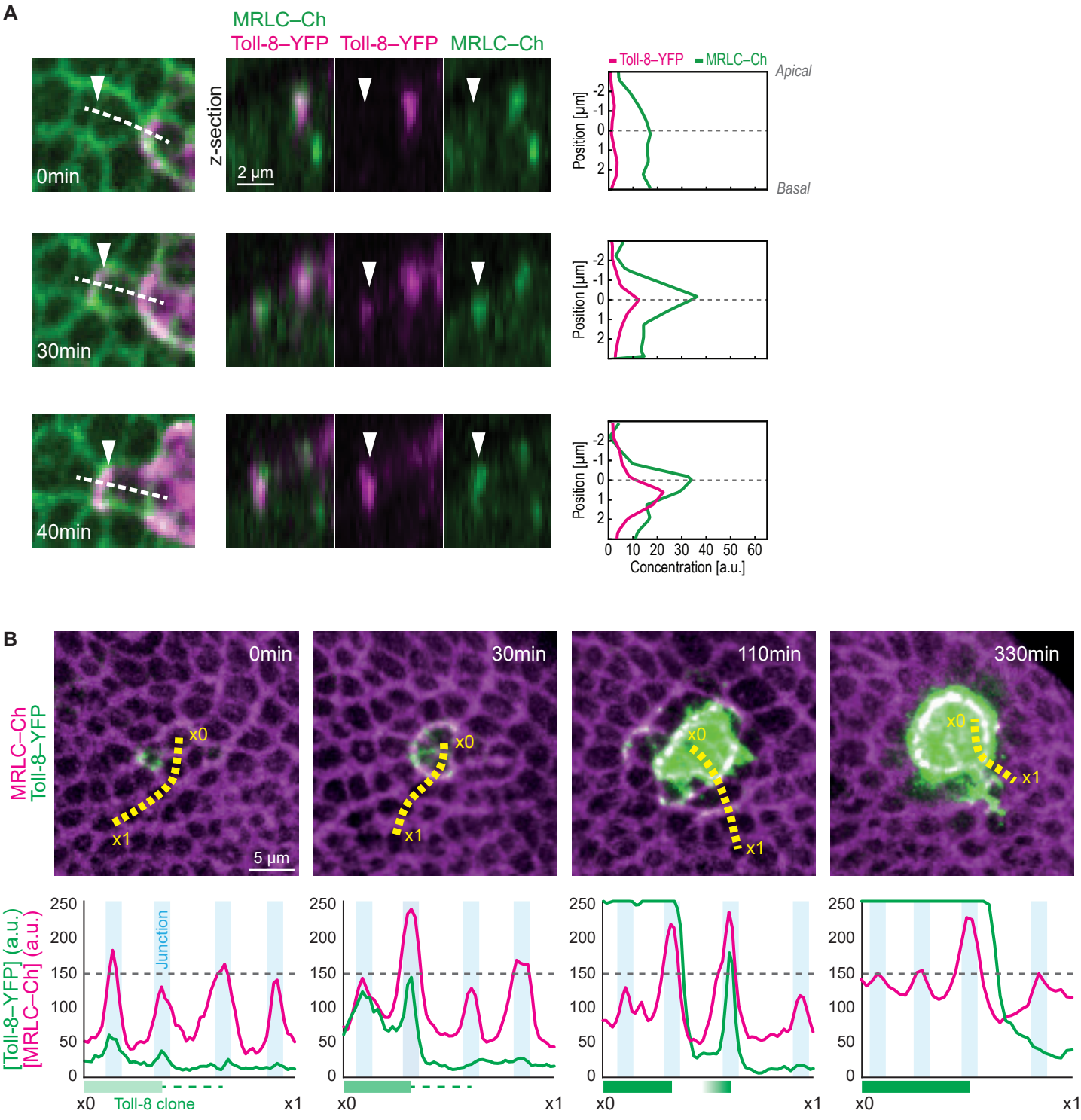
A
MRLC–Ch
Toll-8–YFP Toll-8–YFP MRLC–Ch
z-section
2 µm
0min
30min
40min
Toll-8–YFP
MRLC–Ch
Apical
Basal
Position [µm]
-2
-1
0
1
2
0 10 20 30 40 50 60
Concentration [a.u.]
B
MRLC–Ch
Toll-8–YFP
0min
30min
110min
330min
x0
x1
5 µm
[Toll-8–YFP] (a.u.)
[MRLC–Ch] (a.u.)
250
200
150
100
50
0
Junction
Toll-8 clone

Figure S6. Additional quantifications of nascent Toll-8 overexpressing clones in wing disc movies (related to Figure 6).

(A) Stills from a movie showing a nascent Toll-8–YFP overexpressing clone in a wing disc (left) and corresponding optical cross-sections (middle) at positions indicated by the dashed lines in the left panels. Quantifications (right) of Toll-8–YFP and MRLC–Ch levels along the apicobasal axis of a cell interface (arrowhead) at subsequent time-points in a cell starting to express Toll-8–YFP at t=~0min. Myo-II enrichment is observed when Toll-8–YFP is localized exclusively to cell-cell interfaces (t=30min and 40min).

(B) Quantifications of temporal dynamics of Toll-8–YFP (green) and MRLC–Ch (magenta) at the boundary of a nascent Toll-8–YFP overexpressing clone in the wing disc (panels taken from Figure 6A). Toll-8–YFP and MRLC–Ch levels were quantified along a line (yellow, from x0 to x1) at representative stages of clonal Toll-8 upregulation. Myo-II is enriched at the boundary of Toll-8–YFP expressing cells facing Toll-8–YFP negative cells (middle left). Myo-II is also enriched at interfaces between cells expressing different levels of Toll-8–YFP (middle right) leading to multiple rows of Myo-II enrichment. Once Toll-8–YFP levels equalize between cells, Myo-II only remains enriched at junctions that display differences in Toll-8 expression (right).